Supplementary information

The Dynamics of Plasmon-Induced Hot Carrier Creation in Colloidal Gold

Anna Wach[1,2,3], Camila Bacellar[2], Claudio Cirelli[2], Philip J. M. Johnson[2], Rebeca Gomez Castillo[4], Vitor R. Silveira[5], Peter Broqvist[6], Jolla Kullgren[6], Alexey Maximenko[1], Tomasz Sobol[1], Ewa Partyka-Jankowska[1], Peter Nordlander[7,8], Naomi J. Halas[7,8,9], Jakub Szlachetko[1*], Jacinto Sá[3,5*]

[1] SOLARIS National Synchrotron Radiation Centre, Jagiellonian University, Krakow, Poland

[2] Paul Scherrer Institut, CH-5232 Villigen PSI, Switzerland.

[3] Institute of Physical Chemistry, Polish Academy of Sciences, 01-224 Warsaw, Poland.

[4] Laboratory of Ultrafast X-ray Sciences, École Polytechnique Fédérale de Lausanne (EPFL), 1015 Lausanne, Sweden.

[5] Department of Chemistry-Ångström, Physical Chemistry division, Uppsala University, 751 20 Uppsala, Sweden.

[6] Department of Chemistry-Ångström, Structural Chemistry division, Uppsala University, 751 20 Uppsala, Sweden.

[7]Department of Electrical and Computer Engineering, Rice University, Houston, TX, USA.

[8] Department of Physics and Astronomy, Rice University, Houston, TX, USA.

[9] Department of Chemistry, Rice University, Houston, TX, USA.

* jakub.szlachetko@uj.edu.pl; jacinto.sa@kemi.uu.se

Materials and Methods:

Gold nanoparticles (Au NPs) preparation:

The Au NPs were prepared using the Turkevich method, as outlined by Piella et al.[1] In a brief overview, a 50 mL solution of sodium citrate tribasic dihydrate (6.6 mM) in water was placed in a 100 mL round bottom flask and stirred at 70 °C in an oil bath. Subsequently, 0.1 mL of tannic acid (2.5 mM) was introduced to the reaction mixture. Finally, 1 mL of $HAuCl_4$ (25 mM) was promptly added. Within 5 minutes, the reaction mixture underwent a noticeable colour change from dark blue to wine, confirming the formation of the Au nanoparticles. The synthesised Au nanoparticles were then stored in a refrigerator.

Samples characterisation:

UV-Vis measurements:

The UV-Vis spectra were collected using a Cary 5000 UV-VIS-NIR spectrophotometer.

Dynamic Light Scattering (DLS) measurements:

The DLS data was collected in a Malvern Zetasizer nanoS instrument, and a total of 3 measurements comprised of 12 scans each time was done.

Atomic Force Microscopy (AFM) measurements:

The AFM data was collected on AFM nanosurf with a long Si cantilever in tapping mode with Al reflex.

Steady-state X-ray absorption near-edge structure (XANES):

The steady-state X-ray absorption spectra were collected at the ASTRA beamline of the SOLARIS National Synchrotron Radiation Center[2] in Krakow, Poland. The X-ray beam from the bending magnet (1.3 T) was monochromatised by a double crystal monochromator and focused to a 10 x 1 mm spot size on the sample. The L_3-edge XANES spectra of gold (Au L_3-edge 11919 eV) and platinum (Pt L_3-edge 11564 eV) metal foils were measured in transmission mode with the energy step size of 0.2 eV. Au NPs in aqueous solution were measured in a

custom-made cell in a fluorescence mode using a one-element silicon drift detector (AXAS-M SDD, Ketek).

Standard XAS data reduction steps were performed with Athena software[3]. These include subtraction of pre- and post-edge backgrounds, determining the edge energy, and normalising the data set to an edge jump of 1.

Valence X-ray photoelectron spectroscopy (XPS):

For measurement, the synthesised gold nanoparticles were deposited on the fluorine-doped tin oxide (FTO) glass. Before sample preparation, the glass was cleaned by sonication in a detergent solution, Mili Q water and finally, isopropanol. Subsequently, the Au NPs suspension was mixed with 0.1 M HNO_3 in a 5 µL nitric acid ratio for each 100 µL Au NPs suspension. The cleaned FTO glass was then immersed in the solution overnight. Finally, the samples were dried in argon and annealed at 450°C for 30 min.

The valence band X-ray photoelectron spectra for the gold nanoparticles supported on the FTO glass were measured at the PHELIX beamline[4] of the SOLARIS synchrotron. The spectra were recorded with an electrostatic hemispherical analyser manufactured by SPECS GmbH, PHOIBOS 225, characterised by energy resolution better than 2 meV. XPS measurements were performed under UHV conditions and at room temperature, using monochromatic radiation at a photon energy of 1400 eV with an energy step of 50 meV. Sn *4d* peak was used to normalise the intensity of the spectra collected for Au NPs-FTO sample and the blank FTO. The valence region photoemission spectra were background subtracted with the range recorded for bare FTO.

SwissFEL experiments & data analysis:

The femtosecond X-ray absorption spectroscopy measurements were carried out at the Alvra endstation of the Swiss Free Electron Laser (SwissFEL, Paul Scherrer Institut, Switzerland). The experiment was performed in a PRIME chamber under a helium atmosphere (800 mbar pressure) to maximise X-ray transmission and minimise X-ray scattering noise. The aqueous solution of Au NPs (5 mM) was flown through a capillary to form a 100 µm diameter cylindrical liquid jet with a flow rate of 3-5 ml/min. The jet speed was selected to ensure the sample's renewal between consecutive laser pump/X-ray probe pulses. The liquid sample was pumped

into the chamber by an HPLC pump, retrieved by a catcher system and then pumped out of the experimental chamber back into the sample reservoir by a peristaltic pump.

The sample was optically excited at 532 nm with a pulse duration of approximately 75 fs, generated at a 50 Hz repetition rate by an 800 nm Ti:Sapphire amplified laser system. The pump laser fluence (98 mJ/cm^2) was determined at the beginning of the experiment and chosen to maximise the excited-state fraction while minimising multiphoton absorption effects. The laser beam (focused into 60 x 60 µm^2 spot) and X-ray beam with a spot size of 20 x 20 µm^2, hit the sample in a nearly collinear geometry. The X-ray absorption data were recorded by scanning FEL electron beam energy and the Si(111) monochromator central energies across the Au L_3-edge (in the energy range 11890 – 11950 eV). The X-ray absorption data were recorded by an avalanche photodiode (APD detector) in total fluorescence yield (TFY) mode at approximately 90° from the incident X-ray beam. The fluorescence signal acquired over 5000 shots per energy point was normalised by the incoming X-ray pulse intensity (I0) on a pulse-to-pulse basis. The FEL was running at a repetition rate of 100 Hz, twice the laser pump, allowing for the measurement of consecutive laser-on and laser-off pulses to generate the transient difference signals.

The time scans (temporal traces) are an average of three individual scans collected over several thousands XFEL shots at (11916 eV, 2.5 eV below Au E_F and electrons (11922 eV, 3.0 eV above Au E_F) populations. Following what has been published elsewhere,[5] the time traces were fitted with a monoexponential decay ($D_1(t)$) function described below:

$$D_1(t) = \frac{1}{2} * e^{-\frac{1}{t_1}\left(t - t_0 - {\sigma^2}/{t_1}\right)} * \left[1 + IRF\left(\frac{t - t_0 - {\sigma^2}/{t_1}}{\sqrt{2}\,\sigma}\right)\right] \qquad (eq.\ S1)$$

$$I(t) = a_1 * D_1(t) + C \qquad (eq.\ S2)$$

where $I(t)$ is the intensity of the pump-probe signal at a given time-delay t; t_0 is time-zero; σ is the full-width half maximum (FWHM) of the instrument response function (IRF), a_1 is the pre-exponential factor to the exponential decay time constant with $t_1$time constant and C is a constant offset.

The transient XANES spectra (collected at time delays of 0, 100, 250, and 500 fs) were fitted with two Gaussian distribution peak functions to map signals below and above the Fermi energy. Built-in Gaussian function in Origin Pro (2023b) was used to fit the peaks. The mean energy and width (3σ) distributions of charges (holes) were extracted from the position and FWHM of the Gaussian peak (below the E_F).

$$Gaussian\ funtion: \quad y = y_0 + \frac{A}{\left(w * \left(\sqrt{\left(\frac{\pi}{4 * ln\ (2)}\right)}\right) * e^{\left(\frac{-4*ln(2)*(x-x_c)^2}{w^2}\right)}\right)} \qquad (eq.\ S3)$$

where A is the area, w is the full-width half maximum (FWHM), x_c is the peak center, and y_0 is the base.

Theoretical calculations of Au DOS:

The electronic structure calculations performed in this study were made using the self-consistent-charge density-functional based tight-binding method (SCC-DFTB)[6,7] as implemented in the DFTB+ software package.[8] In the calculations, we used the Slater-Koster tables generated in Ref. 4. This method has been shown to give band structures and electronic properties for different bulk phases and gold clusters (Au_2, Au_8 and Au_{20}) in excellent agreement with plane-wave density functional theory data.[9]

In the current work, we used SCC-DFTB to compute the electronic density of states of the Au bulk and for nanoparticles (NPs) of different sizes and shapes. The bulk Au was calculated using an fcc primitive unit cell sampled using a Monkhorst-Pack k-point grid of 9x9x9 using experimental lattice parameters. The nanoparticles were simulated in a large periodically repeated box tested only at the Gamma point. All structures were first geometry optimised until the maximum force on each atom was smaller than 5 meV/Å, keeping the supercell dimensions fixed.

11 nanoparticles varying from 0.5nm to 3.3 nm in size (13 to 923 Au atoms) were investigated. The density of states (DOS) for these structures is shown in Figure S6. In the figure, it is seen that the DOS is size-dependent for the smaller sizes. However, for the larger ones, the electronic properties converge. Based on these calculations, we have chosen the 3.3 nm Au particle to represent larger Au NPs, which is used in the comparison to experimental data.

Additional data:

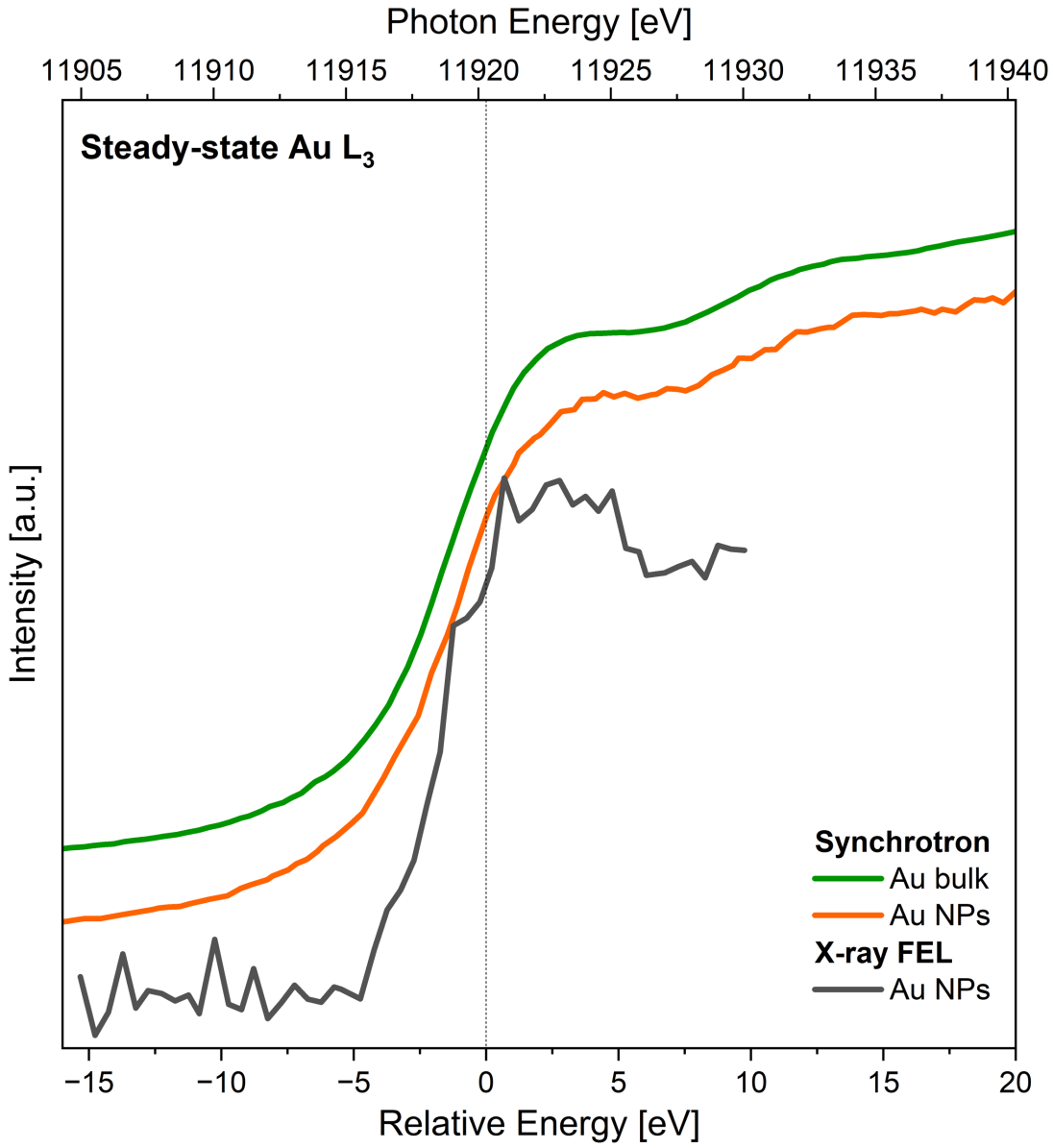

FIGURE S1: Steady-state Au L_3-edge X-ray absorption near edge structure spectra collected for Au foil and nanoparticles at synchrotron and X-ray free-electron laser facilities. The spectra are vertically shifted for clarity.

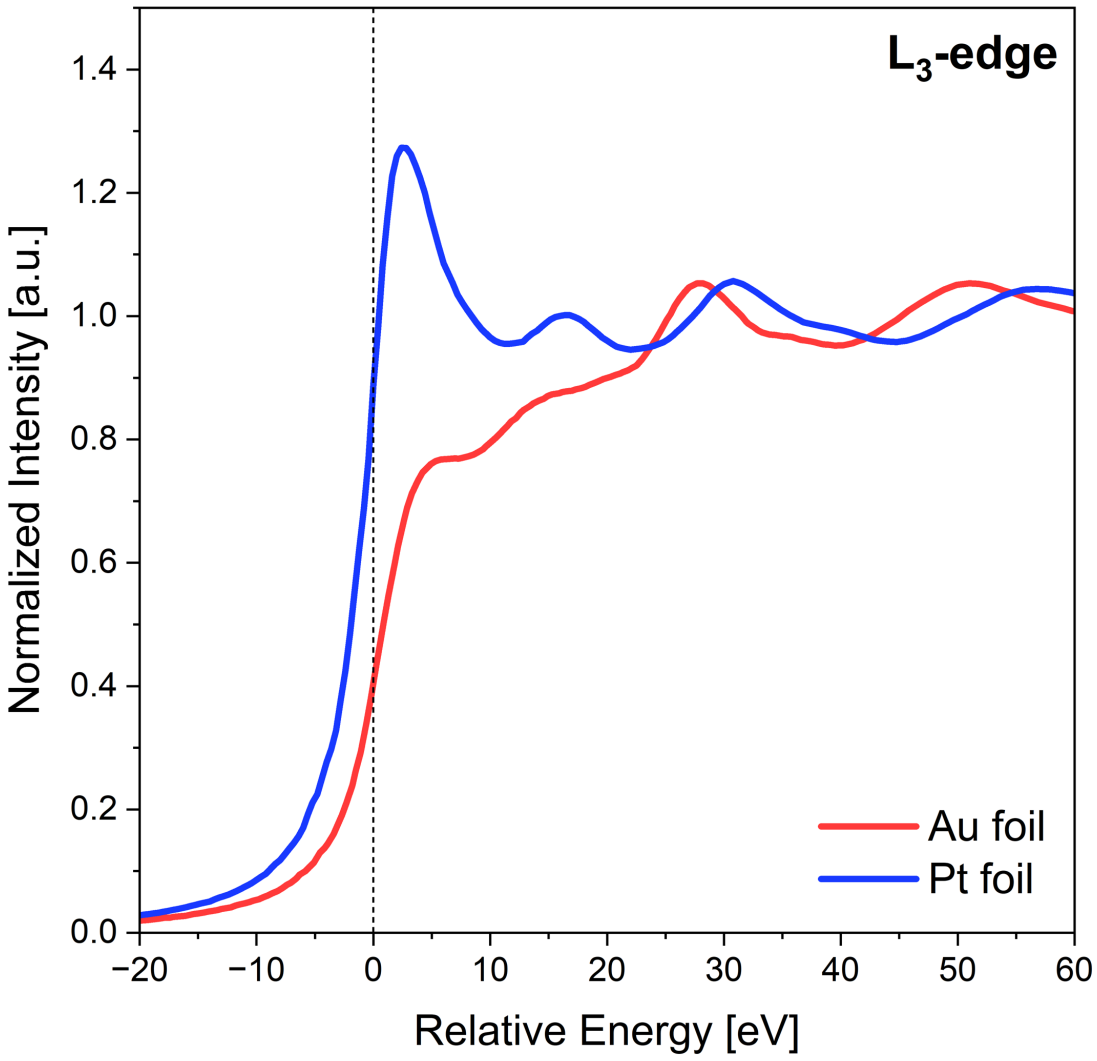

FIGURE S2: L_3-edge XANES of Au and Pt foils overplotted by normalizing the X-axis to the respective Fermi level energy. The inflection point in the edge (marked with a dashed line) was taken as the zero point in the energy scale.

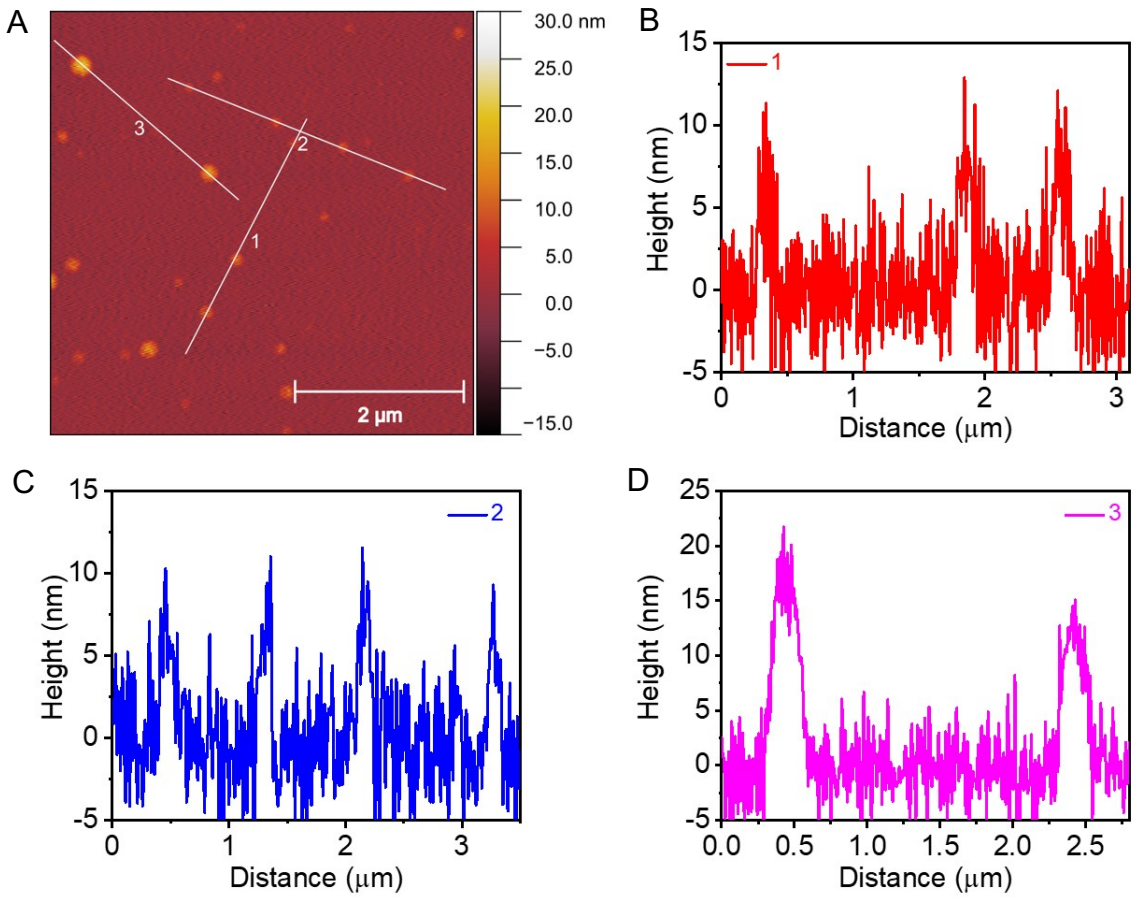

FIGURE S3: AFM of Au NPs on Si after annealing. A) AFM micrograph; and B to D) line tarces showing average particle height.

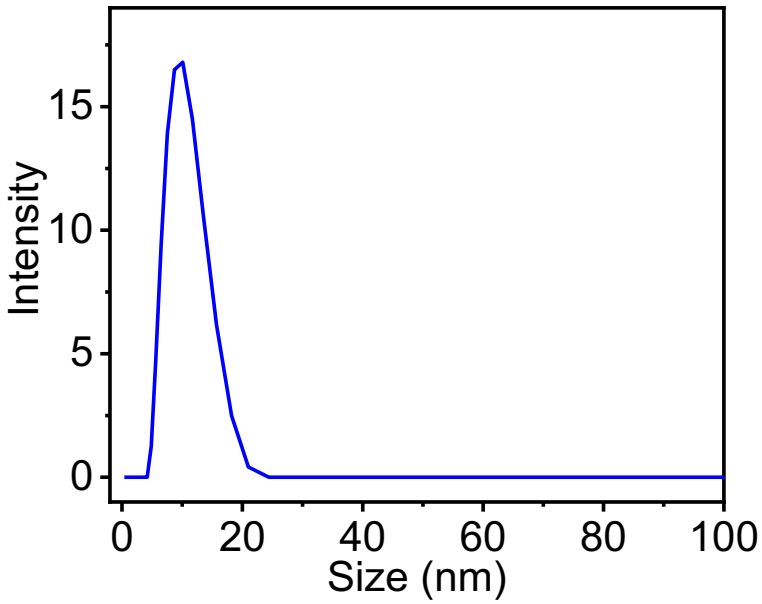

FIGURE S4: Dynamic light scattering (DLS) analysis of Au NPs in water.

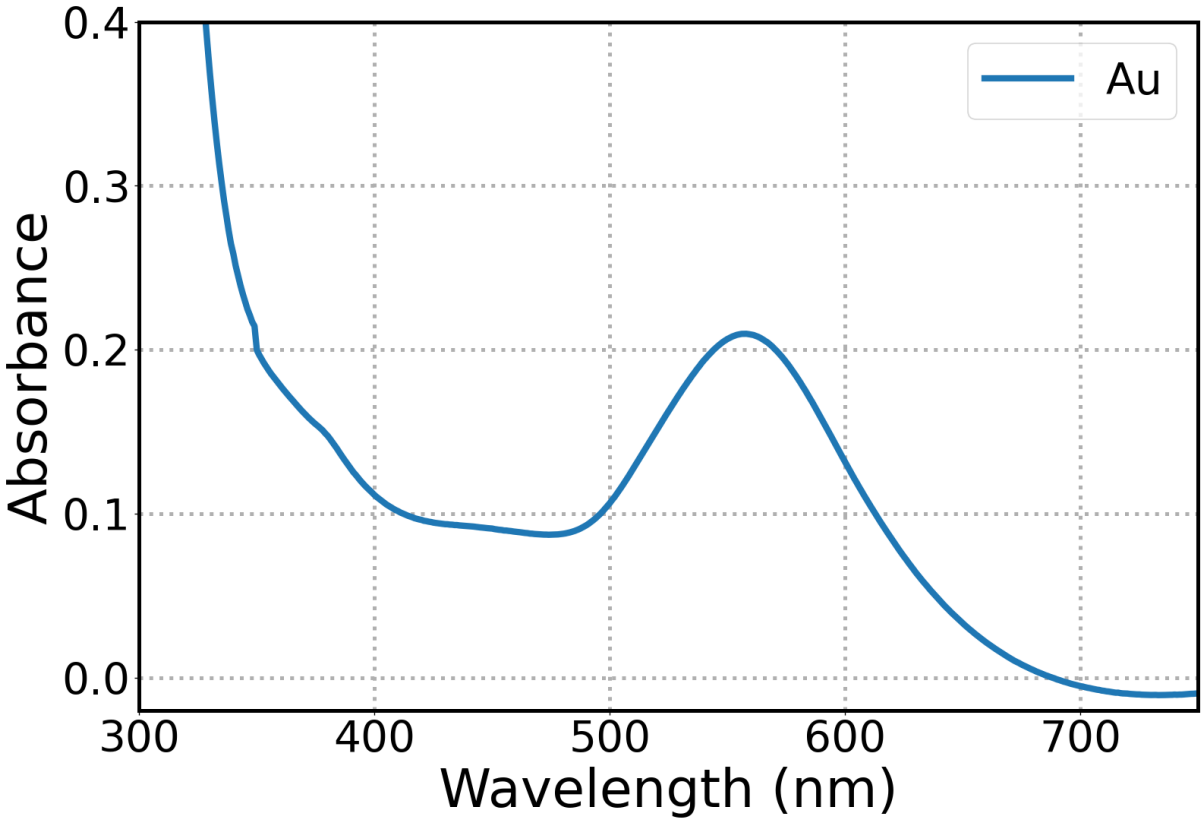

FIGURE S5: Optical absorption of Au NPs in water.

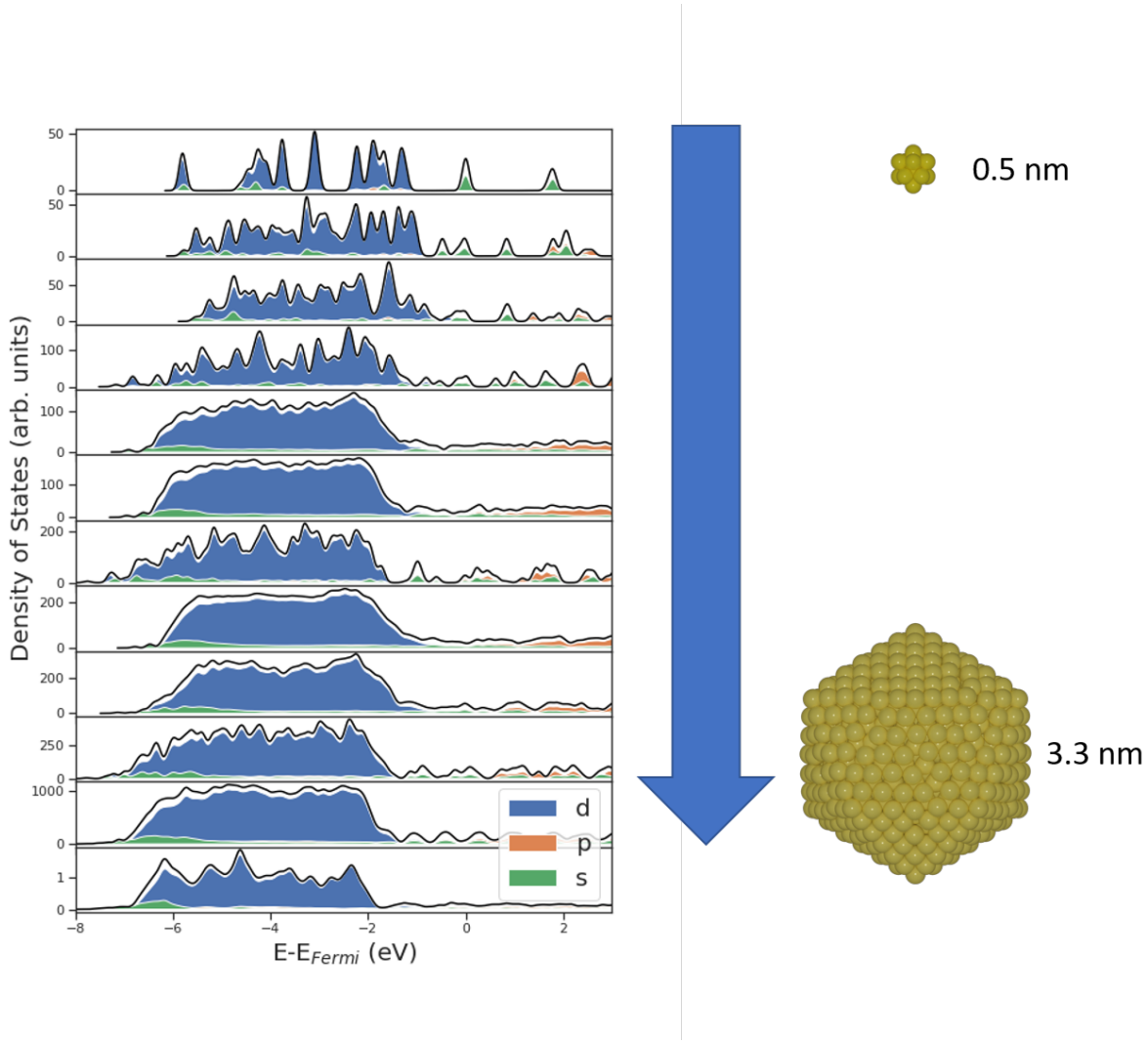

FIGURE S6: Density of states for 11 Au NPs of varying size (DOS for smaller particles at top) and bulk fcc Au (bottom). The smallest and largest NP's, being approximately 0.5 nm and 3.3 nm, respectively, are schematically illustrated in the figure

Supplementary references:

1. Piella, J., Bastús, N. G., Puntes, V. Size-Controlled Synthesis of Sub-10-nanometer Citrate-Stabilized Gold Nanoparticles and Related Optical Properties. *Chem. Mater*. **28**, 1066-5463 (2016).
2. Szlachetko, J., Szade, J., Beyer, E. et al. SOLARIS national synchrotron radiation centre in Krakow, Poland. *Europ. Phys. J. Plus* **138,** 1-10 (2023).
3. Ravel, B., Newville, M. ATHENA and ARTEMIS: Interactive graphical data analysis using IFEFFIT. *Phys. Scr*. **2005**, 1007 (2005).
4. Szczepanik-Ciba, M., Sobol, T., Szade, J. PHELIX–A new soft X-ray spectroscopy beamline at SOLARIS synchrotron. *Nucl. Instrum. Methods Phys. Res., Sect. B* **492**, 49-55 (2021).
5. Bacellar, C., Kinschel, D., Mancini, G. F., Ingle, R. A., Rouxel, J., Cannelli, O., Cirelli, C., Knopp, G., Szlachetko, J., Lima, F. A. et al. Spin cascade and doming in ferric hemes: Femtosecond X-ray absorption and X-ray emission studies. *Proc. Natl. Acad. Sci. USA* **117**, 21914-21920 (2020).
6. Elstner, M., Porezag, D., Jungnickel, G., Elsner, J., Haugk, M., Frauenheim, T., Suhai, S., Seifert, G. Self-consistent-charge density-functional tight-binding method for simulations of complex materials properties. *Phys. Rev. B* **58**, 7260 (1998).
7. Porezag, D., Frauenheim, T., Köhler, T., Seifert, G., Kaschner, R. Construction of tight-binding-like potentials on the basis of density-functional theory: Application to carbon. *Phys. Rev. B* **51**, 12947 (1995).
8. Aradi, B., Hourahine, B., Frauenheim, T. DFTB+, a Sparse Matrix-Based Implementation of the DFTB Method. *J. Phys. Chem. A* **111**, 5678-5684 (2007).
9. Fihey, A., Hettich, C., Touzeau, J., Maurel, F., Perrier, A., Köhler, C., Aradi, B., Frauenheim, T. SCC-DFTB parameters for simulating hybrid gold-thiolates compounds. *J. Comp. Chem.* **36**, 2075-2085 (2015).